Langmuir
Article
pubs.acs.org/Langmuir

Multilevel Self-Aligned Microcontact Printing System

K. Choonee and R. R. A. Syms*

EEE Department, Imperial College London, Exhibition Road, London SW7 2AZ, U.K.

Received March 9, 2010. Revised Manuscript Received July 16, 2010

A multilevel microcontact printing (μCP) system that avoids the use of optical alignment and precision manipulation equipment is demonstrated. Most of the complexity is transferred to the poly(dimethylsiloxane) (PDMS) stamp itself by forming the features, a mechanical self-alignment mechanism, and an elastic membrane by wafer scale replica molding on a Si master. Flexible 50-μm-thick photoetched stainless steel sheets are bonded to PDMS prior to demolding to improve the mechanical stability. The Si master itself is made using conventional MEMS fabrication tools such as photolithography, reactive ion etching, and anisotropic wet etching. Self-alignment is achieved by introducing protrusions on the stamp that mate onto corresponding grooves on a machined substrate. Complete 10 mm $\times$10 mm prototypes are fabricated, and six-level μCP is demonstrated with an average layer-to-layer misalignment of 5−10 μm.

1. Introduction

μCP is a simple, low-cost patterning method offering submicrometer accuracy and versatility that was initially demonstrated by Whitesides and co-workers in 1993.[1] The starting point is a soft elastomeric stamp carrying raised patterns, which is inked and then brought into contact with an appropriate substrate. The ink then spontaneously forms self-assembled monolayers (SAM) on the substrate in the regions corresponding to the raised features of the stamp. Typically, the stamp is made of poly(dimethylsiloxane) (PDMS), which is cast on a microfabricated silicon master, the ink is an alkanethiol of the form $SH(CH_2)_nCH_3$ (with $n > 11$), and the substrate is Au.

Since the initial demonstration,[1] μCP has improved tremendously. For example, feature sizes have been shrunk to the nanometer (down to 50 nm) regime by the development of new materials[2] and multilayer stamps.[2,3] Schemes for large-area printing, motivated by the development of flexible electronics, have been devised.[4−7] Suitable inks and substrate combinations have also been thoroughly investigated, and most metals and technologically important semiconductors can be patterned. (See Love et al.[8] and Smith et al.[9] for a review of ink/substrate combinations.) In addition, modifying the surface properties of PDMS stamps to accommodate for polar inks has been demonstrated.[10] A host of other improvements have been developed to push the limits of μCP even further.[11−13]

Applications of μCP lie in both biochemistry and microfabrication. However, there is far more interest in biochemistry because the surface and chemical properties of the patterned monolayer can be tailored by changing the headgroup. One key area is the patterning of proteins to control and investigate cell behavior.[14−19] Typically, a first hydrophobic layer is deposited by μCP to form adhesive islands for proteins, and a second hydrophilic SAM is formed from solution in the empty areas to provide a nonfouling surface. Clearly, if more levels of SAMs could be patterned with accurate control of the geometry, then the surface properties could be differentiated even further.

The problem of alignment appears again in in vitro studies of neurons[20−22] where the stamps need to be aligned to microstructured electrodes.[23,24] Currently, alignment is carried out using customized systems that combine three-axis stages to an optical microscope. This setup, however, may become cumbersome where multilevel μCP is required or where there is no optical access.

Despite the clear need for equipment for μCP, few commercial solutions (e.g., the μCP 2.1,[25] GeSiM, Grosserkmannsdorf, Germany) exist and many are arguably too expensive and complicated[4−7] for use outside the microelectronics industry.

*Corresponding author. E-mail: r.syms@imperial.ac.uk.

(1) Kumar, A.; Whitesides, G. M. *Appl. Phys. Lett*. **1993**, *63*, 2002–2004.
(2) Schmid, H.; Michel, B. *Macromolecules* **2000**, *33*, 3042–3049.
(3) Odom, T. W.; Love, J. C.; Wolfe, D. B.; Paul, K. E.; Whitesides, G. M. *Langmuir* **2002**, *18*, 5314–5320.
(4) Rogers, J. A.; Bao, Z.; Baldwin, K.; Dodabalapur, A.; Crone, B.; Raju, V. R.; Kuck, V.; Katz, H.; Amundson, K.; Ewing, J.; Drzaic, P. *Proc. Natl. Acad. Sci. U.S.A*. **2001**, *98*, 4835–4840.
(5) Burgin, T.; Choong, V. E.; Maracas, G. *Langmuir* **2000**, *16*, 5371–5375.
(6) Decre, M. M. J.; Schneider, R. M.; Burdinski, D.; Schellekens, J.; Saalmink, M.; Dona, R. *Mater. Res. Soc. Symp. Proc*. **2004**, *M4*, 9.
(7) Delamarche, E.; Vichiconti, J.; Hall, S. A.; Geissler, M.; Graham, W.; Michel, B.; Nunes, R. *Langmuir* **2003**, *19*, 6567–6569.
(8) Love, J. C.; Estroff, L. A.; Kriebel, J. K.; Nuzzo, R. G.; Whitesides, G. M. *Chem. Rev*. **2005**, *105*, 1103–1170.
(9) Smith, R. K.; Lewis, P. A.; Weiss, P. S. *Prog. Surf. Sci*. **2004**, *75*, 1–68.
(10) Delamarche, E.; Donzel, C.; Kamounah, F. S.; Wolf, H.; Geissler, M.; Stutz, R.; Schmidt-Winkel, P.; Michel, B.; Mathieu, H. J.; Schaumburg, K. *Langmuir* **2003**, *19*, 8749–8758.
(11) Quist, A. P.; Pavlovic, E.; Oscarsson, S. *Anal. Bioanal. Chem*. **2005**, *381*, 591–600.
(12) Perl, A.; Reinhoudt, D., N.; Huskens, J. *Adv. Mater*. **2009**, *21*, 2257–2268.
(13) Rogers, J. A.; Nuzzo, R. G. *Mater. Today* **2005**, *8*, 50–56.
(14) Whitesides, G. M.; Ostuni, E.; Takayama, S.; Jiang, X.; Ingber, D. E. *Ann. Biomed. Eng*. **2001**, *3*, 335–373.
(15) Mrksich, M.; Whitesides, G. M. *Trends Biotechnol*. **1995**, *13*, 228–235.
(16) Mrksich, M.; Dike, L. E.; Tien, J.; Ingber, D. E.; Whitesides, G. M. *Exp. Cell. Res*. **1997**, *235*, 305–313.
(17) Mrksich, M.; Chen, C. S.; Xia, Y.; Dike, L. E.; Ingber, D. E.; Whitesides, G. M. *Proc. Natl. Acad. Sci. U.S.A*. **1996**, *93*, 10775–10778.
(18) Brock, A.; Chang, E.; Ho, C.-C.; LeDuc, P.; Jiang, X.; Whitesides, G. M.; Ingber, D. E. *Langmuir* **2003**, *19*, 1611–1617.
(19) Chen, C. S.; Mrksich, M.; Huang, S.; Whitesides, G. M.; Ingber, D. E. *Biotechnol. Prog*. **1998**, *14*, 356–363.
(20) St. John, P. M.; Kam, L.; Turner, S. W.; Craighead, H. G.; Issacson, M.; Turner, J. N.; Shain, W. *J. Neurosci. Methods* **1997**, *75*, 171–177.
(21) Scholl, M.; Sprössler, C.; Denyer, M.; Krause, M.; Nakajima, K.; Maelicke, A.; Knoll, W.; Offenhäusser, A. *J. Neurosci. Methods* **2000**, *104*, 65–75.
(22) Oliva, A. A.; James, C. D.; Kingman, C. E.; Craighead, H. G.; Banker, G. A. *Neurochem. Res*. **2003**, *28*, 1639–1648.
(23) James, C. D.; Davis, R.; Meyer, M.; Turner, A.; Turner, S.; Withers, G.; Kam, L.; Banker, G.; Craighead, H.; Issacson, M.; Turner, J.; Shain, W. *IEEE Trans. Biomed. Eng*. **2000**, *47*, 17–21.
(24) Lauer, L.; Ingebrandt, S.; Scholl, K.; Offenhauer, A. *IEEE Trans. Biomed. Eng*. **2001**, *48*, 838–842.
(25) GeSIM Micro-Contact Printing Instruments. http://www.gesim.de

Although stamps can be cleaned, reinked, and reused, they cannot be completely cleaned of ink and, for some applications, must be changed frequently to avoid cross contamination. Hence, there is a need to develop low-cost disposable stamps that have self-alignment features (to avoid the need for further external equipment).

In this article, we present a soft lithographic solution consisting of PDMS stamps that can be used for self-aligned multilevel printing, based on membrane-like stamps that are designed to interlock mechanically with target substrates. Bilevel etched Si masters are used to form the patterns and the mechanical features (the suspension and alignment) by replica molding, and Au-coated target substrates with corresponding mechanical features are made by anisotropic etching of crystalline Si. Some of these concepts have been demonstrated on silicon.[26] Currently, printing is carried out by manually deflecting the stamp to make contact, but other more controlled actuation mechanisms such as electrostatic and pneumatic could also be implemented with relative ease.

Section 2 outlines the concept and describes the in-depth design of the dies. Finite element analysis (FEA) is also carried out to verify the device behavior. Section 3 presents a wafer-scale fabrication process for 100 mm wafers carrying 36 dies. Results and demonstration of aligned six-level μCP are illustrated in section 4, and conclusions are presented in section 5.

2. Concept and Design

In this section, the PDMS μCP system is described. Replica molding is used to cast membrane-like PDMS devices on microfabricated 100 mm Si⟨100⟩ wafers. Each die is ca. 10 mm $\times$10 mm and carries alignment features, the pattern to be printed, and a suspension in the form of a membrane. The geometry of the alignment features and the pattern are determined by the bilevel etched silicon, and the thickness of the membrane is determined by the thickness of the PDMS. We start by explaining the self-alignment mechanism, followed by a discussion of the elastic backing. Pattern stability and the mechanical properties of the stamp are investigated through FEA. Finally, the use of different patterns on the wafer to enable the characterization of multilevel accuracy is described.

2.1. Self-Alignment. Self-alignment is achieved by micromachining a Si⟨100⟩ target substrate to form complementary V grooves that mate with V-shaped rails on the stamp. This interlocking mechanism has been demonstrated previously[26,27] and is illustrated in Figure 1. With crystalline Si⟨100⟩, θ is the angle between the (100) and (111) planes and $\tan(\theta) = (2)^{1/2}$. The flying height, S, then depends on the groove widths on the substrate, W_T, and on the stamp, W_M, where $S = (W_M - W_T)/(2)^{1/2}$. Here, $W_M = 1000\,\mu$m and $W_T = 930\,\mu$m, giving $S = 50\,\mu$m. When the rail and groove are tall/deep enough (200 μm in this case), the male and female parts can easily be aligned and registered by hand. Because of the elastomeric nature of the male part, some misalignment is expected.

2.2. Elastic Backing. The softness of PDMS, typically 1 to 2 MPa, is critical because it enables conformal contact but also makes stamp handling and registration very difficult. The stress induced by the thermal curing process adds further complications, especially because the PDMS stamp needs to be aligned to Si substrates. Therefore, an elastic backing to strengthen the stamp is included.

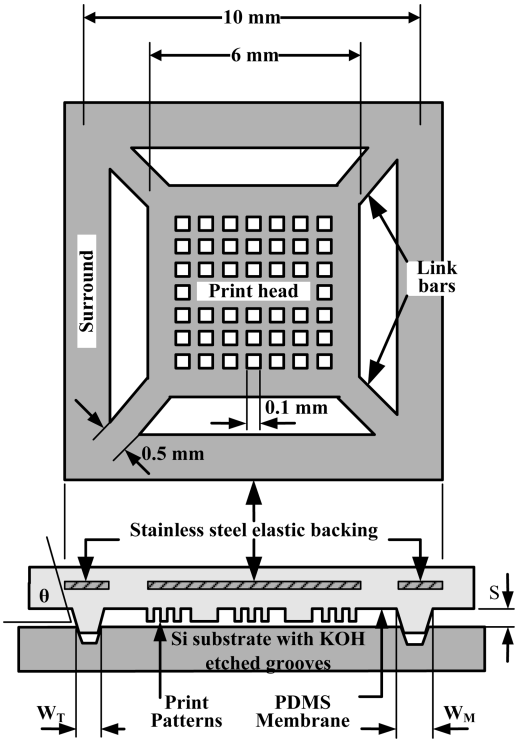

Figure 1. Self-aligned μCP system. The upper image shows the plan view of the steel elastic backing, and the lower image shows the cross-sectional view of the device showing self-alignment.

A stamp cured at ~100 C shrinks by 1.5% (in a linear dimension)[28] when it is released from a hard master such as Si, and a solution is to bond a flexible but stiff backing layer[29] prior to demolding. We have experimentally verified this by using layers such as 50 μm stainless steel sheets, 25−100 μm Kapton polyimide sheets, and overhead transparencies and have found that the shrinkage is reduced to 0.1%.

Furthermore, as the stamp is deflected to make contact, it is expected to stretch and distort. By locally stiffening the print head area and the alignment rail and allowing the membrane region to stretch instead, pattern distortion is minimized. This is done by bonding a 50-μm-thick photoetched stainless steel sheet (Photofab Ltd., Cambridgeshire, U.K.) to the PDMS after casting. The layout of the patterned elastic backing and its position in the PDMS stamp are illustrated in Figure 1. The surround overlays the PDMS alignment rail and ensures dimensional stability, and the steel print head strengthens the print pattern region and keeps it flat. The link bars hold all of it together and ensure that the stamp retracts after contact, while the 100 μm square holes on the steel print head allow trapped bubbles to escape during the fabrication process.

2.3. Pattern Stability. Because of its softness, PDMS patterns are prone to collapse during printing.[30−32] With a feature height (10 μm) to width (10 μm) ratio of unity, pattern buckling or pairing is avoided but roof collapse, which occurs when features are widely spaced from each other, could be a problem.

(26) Syms, R. R. A.; Zou, H.; Choonee, K.; Lawes, R. A. *J. Micromech. Microeng.* **2009**, *19*, 025027.
(27) Larsson, M. P.; Syms, R. R. A. *J. Microelectromech. Syst.* **2004**, *13*, 365.
(28) Govindaraju, A.; Chakraborty, A.; Luo, C. *J. Micromech. Microeng.* **2005**, *15*, 1303–1309.
(29) Moraes, C.; Sun, Y.; Simmons, C. A. *J. Micromech. Microeng.* **2009**, *19*, 065015.
(30) Hui, C. Y.; Jagota, A.; Lin, Y. Y.; Kramer, E. J. *Langmuir* **2002**, *18*, 1394–1407.
(31) Delamarche, E.; Schmid, H.; Michel, B.; Biebuyck, H. *Adv. Mater.* **1997**, *9*, 741–746.
(32) Decre, M. M. J.; Timmermans, P. H. M.; van der Sluis, O.; Schroeders, R. *Langmuir* **2005**, *21*, 7971–7978.

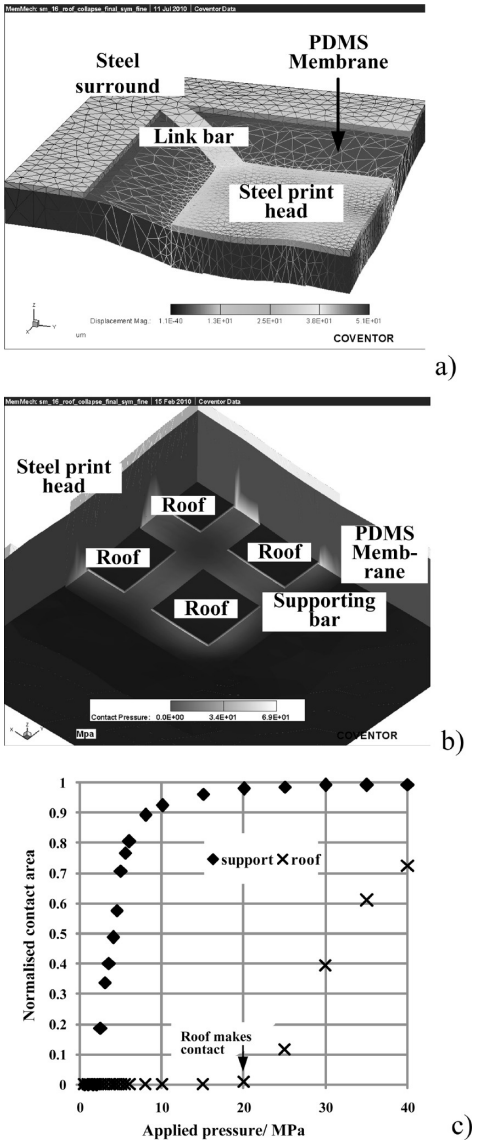

Figure 2. FEA of stamp. (a) Deflection profile for an applied load of 20 MPa. (b) Contact pressure on the underside of the stamp for a load of 20 MPa. (c) Normalized contact area variation with applied load.

One solution, apart from avoiding sparse areas, is to use flexible backing layers.[33] Here, both measures are implemented by including 500 μm supporting bars that surround the patterns and by using a flexible stainless steel backing. The effectiveness of the supporting bars is elaborated further in section 2.4.

In addition, submicrometer features can be patterned by using composite stamps as described in earlier reports.[2,3] To test these, we use a different master carrying 500-nm-wide gaps with a pitch of 5 μm in 7 μm tall posts. The layouts of these masters are described in section 2.5, and fabrication is explained in section 3.

2.4. Simulation. The mechanical response of the stamp and the interaction with the substrate are investigated via FEA in the CoventorWare software. Exploiting the symmetrical geometry, only one-fourth of the device is simulated, with the symmetry planes constrained in the x or y plane as required. A uniform pressure is applied to the top of the metal plate, and the outer edges of the stamp and the surrounding metal are fixed.

The simulated model under a load of 20 MPa is illustrated in Figure 2a and excludes the print patterns, the 100 μm square holes in the steel plate, and the PDMS alignment ridge. Contact is modeled by including a contact surface 50 μm below the roof of the stamp. The membrane areas bend more, with the metal-bound region staying mostly flat. Contact is illustrated in Figure 2b, which shows that the full length of the supporting bar can be in contact with the substrate without any contact of the roof. This implies that the patterns, which are of the same height, would also make contact. The variation of the normalized contact area of the supporting bars and of the roof with the applied load is plotted in Figure 2c, showing that essentially full contact of the print patterns can be achieved without roof collapse.

Although not simulated per se, the retraction of the stamp after contact can be predicted. Considering the deflection of the print head with varying loads (data not shown) for deflections of up to 40 μm (i.e., prior to contact being made), the relationship is linear. From the gradient of the linear part, a stiffness term can be estimated (k = 50 kN/m). The maximum displacement that this node can undergo is S_0 = 40 μm. Hence, the elastic energy stored ($= kS_0^2/2$) is at least 40 μJ (because even more energy is stored as the stamp deforms during contact). On the other hand, the work required to release the stamp is given by the product of the area in contact and the work of adhesion, W. Here, the relevant value of W to use is that of Sylgard 184 on gold,[34] which is 0.5 J/m^2, and the total area in contact is approximated by the area of the bottom surface of the supporting bars, which is 4.6×10^{-6} m^2. The adhesion energy is thus 2.3 μJ. Because the stored elastic energy is much greater than the adhesion energy, stiction is not expected to be a problem.

2.5. Stamps and Patterns for Multilevel Characterization. To test for overlay accuracy, seven stamps carrying different patterns are made from the same silicon wafer. Variants are labeled #1 − #6 and "all", and their layout on the wafer is illustrated in Figure 3a. Each variant contains the same mechanical features (alignment, supports, and suspension) but different patterns. The variants consist of a 3 × 3 array of identical cells of size 1.2 mm × 1.2 mm, with each cell containing an identical periodic pattern of ten 10-μm-wide vertical bars with a pitch of 20 μm and 10-μm-wide horizontal bars for identification, as illustrated in Figure 3b. The 3 × 3 array of cells carrying the patterns is surrounded by 500-μm-wide supports, and together they form the 5.6 mm × 5.6 mm printed area. The print head itself lies in a membrane-like structure framed by 10 mm × 10 mm alignment rails. The variants differ only in the position of the periodic bar pattern within each cell, as illustrated in Figure 3c, which shows that the pattern carried by each variant is laterally shifted by an amount depending on the variant number. Sequentially printing with variants 1−6 and comparing the measured separation with the designed value allows multilevel accuracy to be measured.

In addition, a different silicon master carrying the same mechanical features but different print patterns was fabricated to test the submicrometer patterning. The print patterns in this case consist of 7-μm-tall periodic bar patterns of different sizes, namely, 10 μm bars with 20 μm pitch, 5 μm bars with 10 μm pitch, and 2.5 μm bars with 5 μm pitch. During processing, the 2.5 μm bars are narrowed to 500 nm by oxidation and subsequent oxide removal. This results in a PDMS stamp having 4.5 μm bars separated by 500 nm gaps.

3. Fabrication

A wafer-scale process for the fabrication of the master and target is presented. Wafer-scale PDMS casting and bonding are discussed, and limitations of the process are outlined.

(33) Menard, E.; Bilhaut, L.; Zaumseil, J.; Rogers, J. A. *Langmuir* **2004**, *20*, 6871–6878.

(34) Bietsch, A.; Michel, B. *J. Appl. Phys.* **2000**, *88*, 4310–4318.

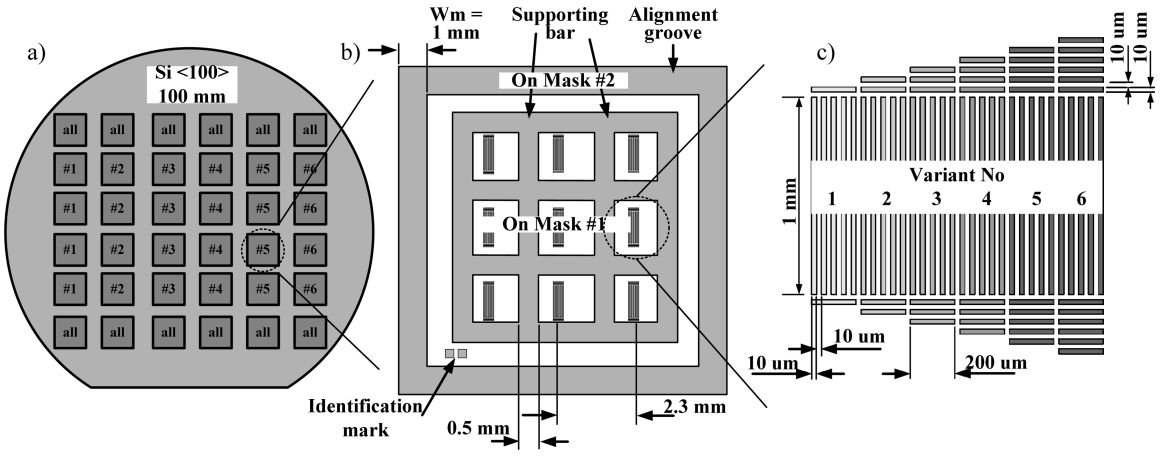

Figure 3. (a) Multiple stamps on a single silicon wafer. (b) Schematic of a single die showing 3×3 cells containing the print pattern, the supporting bar (mask no. 1), and the alignment groove (mask no. 2). (c) Close-up of the pattern. Variants carry the same periodic bar pattern, but it is shifted laterally (e.g., variant no. 1 carries the leftmost group, variant no. 2 carries the second group from the left, and so on). Variant "all" carries all six groups.

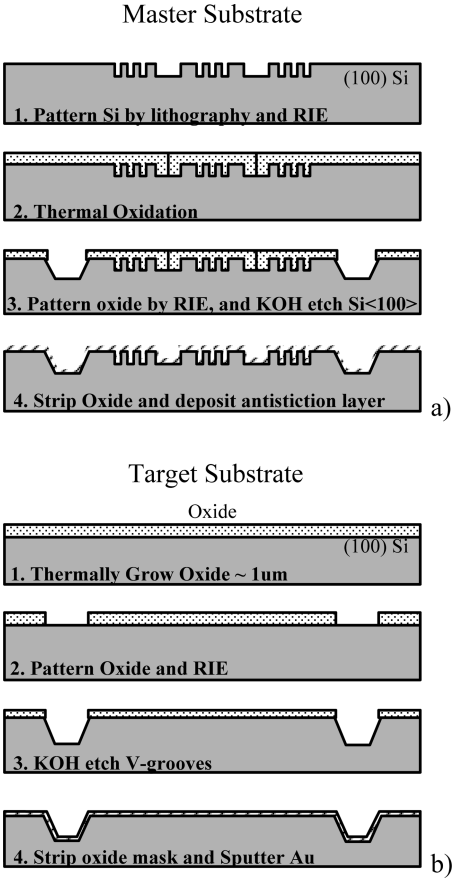

Figure 4. (a) Master and (b) target fabrication processes.

3.1. Master and Target. The master and target substrate are fabricated by conventional MEMS fabrication techniques using two-level lithography for the master and single-level lithography for the target. The process flows are illustrated in Figure 4a,b. Both the master and target carry 36 dies. In the case of the target, the dies are identical, but for the master, the dies correspond to different variants. The masters carrying the fine 2.5 μm patterns are made with the same process flow but with adjustments to the first lithography step.

For the master, the print patterns and the supporting posts are defined in a single mask (mask #1) and transferred to the Si

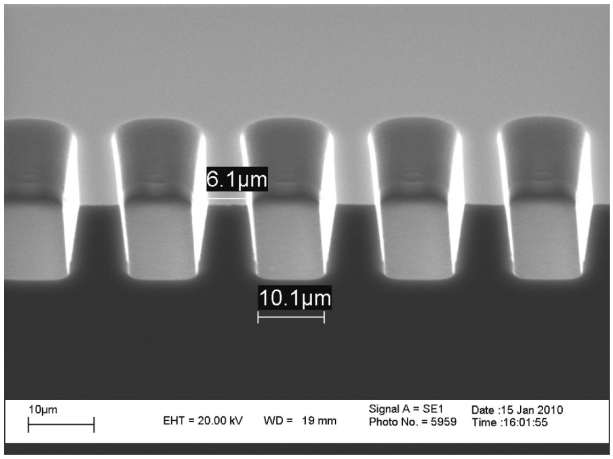

Figure 5. Cross section of the 10 μm periodic bar patterns on the completed master.

substrate by a RIE (System 80, Oxford Instruments) to a depth of 10 μm using an SF_6 (30 sccm) and O_2 (10 sccm) gas mixture at a base pressure of 120 mTorr and an rf power of 100 W. This recipe yields a slightly tapered sidewall (~10° with respect to the normal) that facilitates demolding. A cross-sectional view of the etched pattern is shown in Figure 5. A 1.2-μm-thick oxide layer is then grown by dry oxidation at 1100 °C on both the microstructured master and the target. A thick 17 μm resist layer (AZ9260, MicroChem) is then spun on the master to cover the shallow structures, and a thinner resist layer is used for the flat target. The master is patterned with mask #2 to define the 1000-μm-wide groove, and the target is patterned with mask #3 to define the 930-μm-wide mating grooves. The patterns are transferred to the oxide mask by RIE (rf power = 200 W, base pressure = 30 mTorr, CHF_3 = 25 sccm, Ar = 25 sccm, and O_2 = 2 sccm). Using the oxide layer as a mask, the Si master and target are then etched in a 40% KOH solution at 80 °C up to a depth of 200 μm. The oxide mask is then stripped, and for the master, an antistiction layer, such as the passivation layer of a DRIE (STS, Newport, U.K.), is deposited, whereas the target is sputter coated with a 30 nm Au layer. The passivated master could be used for ~10 PDMS moldings/castings before the release layer deteriorated and needed to be redeposited.

Note that at the convex corners additional ⟨211⟩ planes are revealed so the grooves are not precisely V-shaped there. To ensure a good

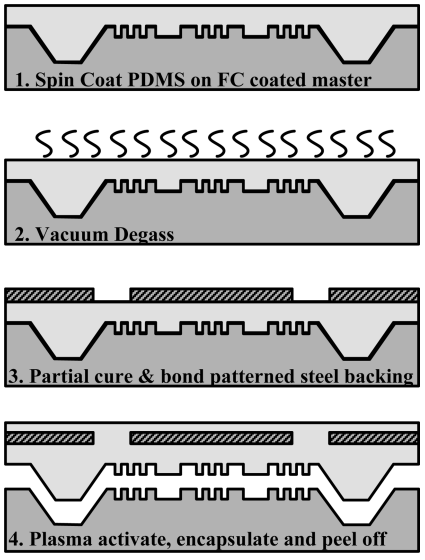

Figure 6. Stamp-replication process.

fit between the stamps and the targets, both the target and master substrates are etched together and to the same depth.

3.2. PDMS Stamp Casting. The stamp-replication process is illustrated in Figure 6. A standard PDMS composition, Sylgard 184 (Dow Corning Corp), is prepared and deposited onto the master via spin coating to form an ~200-μm-thick PDMS layer. After spinning, the master is degassed in a desiccator to remove air bubbles. The PDMS is then partially cured so that it is set and does not flow but is still sticky.

For submicrometer features, composite PDMS stamps with a 30 μm hard layer of Sylgard 184 mixed with its modulator in a ratio of 1:5, followed by a 200-μm-thick layer in a 1:10 formulation, were made. The remainder of the stamp-casting process is identical. This "hard" 1:5 layer is reported[35] to have an ultimate tensile strength that is 50% that of conventional 1:10 Sylgard 184, and this initial test indicates that the stamp-replication process is suitable for brittle PDMS.

The patterned steel layer is then bonded onto the PDMS. Alignment is carried out by using the alignment optics of a mask aligner (Quintel Q4000IR) with the PDMS-coated substrate held on the wafer stage and the steel sheet (which is first mounted on a glass plate) held on the mask chuck. To avoid stiction during the precontact phase, the PDMS curing time had to be increased; consequently, the PDMS−steel bond weakened significantly, and the yield was quite poor. This aspect can be improved on with a contact aligner system where the precontact phase can be overridden.

Alternatively, the steel sheet is cut into strips covering 2 × 6 or 1 × 6 dies and coarsely aligned by hand using the alignment grooves as a guide. Fewer dies are obtained per wafer with this method, but the dies are of better quality.

After bonding, a release layer in the form of a flexible polycarbonate sheet (such as an overhead transparency) is placed on top of the steel sheet, followed by a blank silicon wafer and a 1.2 kg weight. The whole assembly is cured on a hot plate for at least 1 h at 90 °C. After cooling, the top Si wafer and the polycarbonate sheet are removed and the stainless steel surface is plasma activated and a second (~200 μm) PDMS layer is spun cast on top and then cured to encapsulate the device.

Finally, the entire PDMS device is peeled off from the master and cut with sharp scissors into individual dies. Figure 7a shows

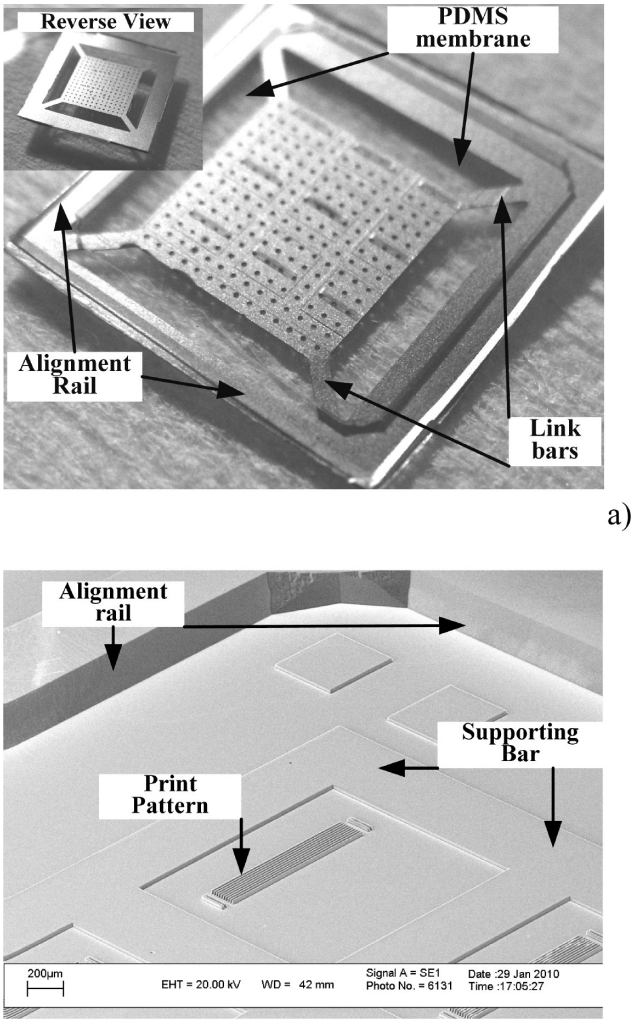

Figure 7. (a) Optical image of a completed stamp. (b) SEM of a finished die highlighting successful molding.

an optical image of a fully assembled stamp, and Figure 7b shows a scanning electron micrograph of the polymer part.

4. Results and Discussion

In this section, the inks and etchants used to carry out μCP are described, six-level patterning is demonstrated, and the resulting layer-to-layer accuracy is presented and discussed. Printing with different inks is also verified.

4.1. Experimental Method. μCP was carried out using a 0.5 mM solution of 1-hexadecanethiol ($HS(CH_2)_{15}CH_3$) in ethanol, which forms well-ordered SAMs on Au. The stamps were coated with the ink and then blown dry. The stamps were aligned by hand onto a site on the target substrates, and to ensure uniform loading, an ~6 mm × 6 mm piece of Si was placed over the print head. Contact was made by pressing the print head with tweezers and was maintained for ~30 s. The SAM pattern was then transferred to Au by etching in a solution of potassium thiosulphate ($K_2S_2O_3$, 0.1 M), potassium hydroxide (KOH, 1 M), and potassium ferricyanide ($K_3Fe(CN)_6$, 0.01 M), which attacks the exposed Au but not the SAM-derivatized regions. Scanning electron microscopy (SEM) was carried out on the etched Au/Si samples to visualize the pattern. To characterize large areas, an optical microscope (Wyko NT9100) with a calibrated $x-y$ stage (±5 μm) was used.

(35) Mata, A.; Fleischman, A.; Roy, S. *Biomed. Microdev.* **2005**, *7*, 281–293.

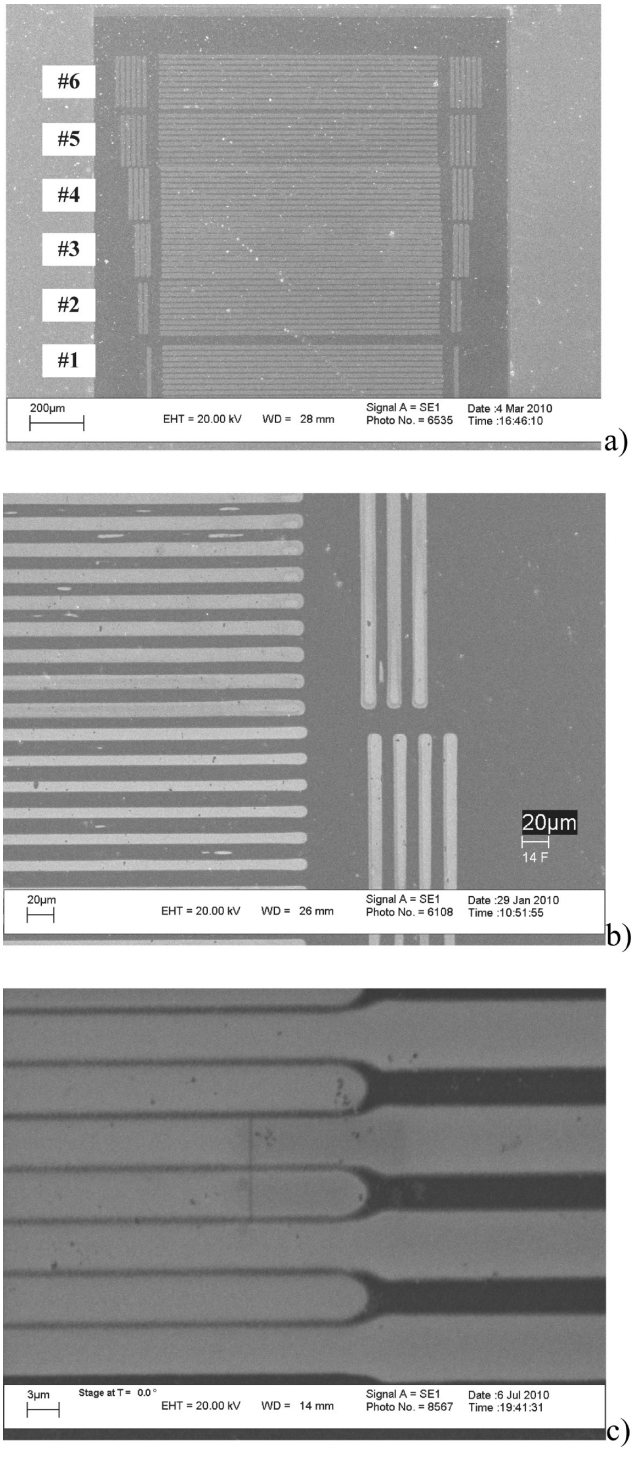

Figure 8. Experimental results of μCP. (a) Six-level μCP. (b) Close-up showing small misalignment between prints of adjacent stamps. (c) Submicrometer patterns.

4.2. Six-Level μCP. Six-level μCP was carried out by inking and sequentially aligning each stamp and making contact. Correlated stamps, that is, those made on a single wafer and bound with the same strip of steel, were used for these experiments. After all six prints were made, the target die was etched to reveal the pattern via SEM imaging. Typical results are illustrated in Figure 8a,b. Submicrometer patterning was carried out in the same way, and the results are illustrated in Figure 8c although no alignment data is presented in this article.

The pattern reproducibility of the stamps carrying 10 μm features is characterized by measuring the absolute distortion,

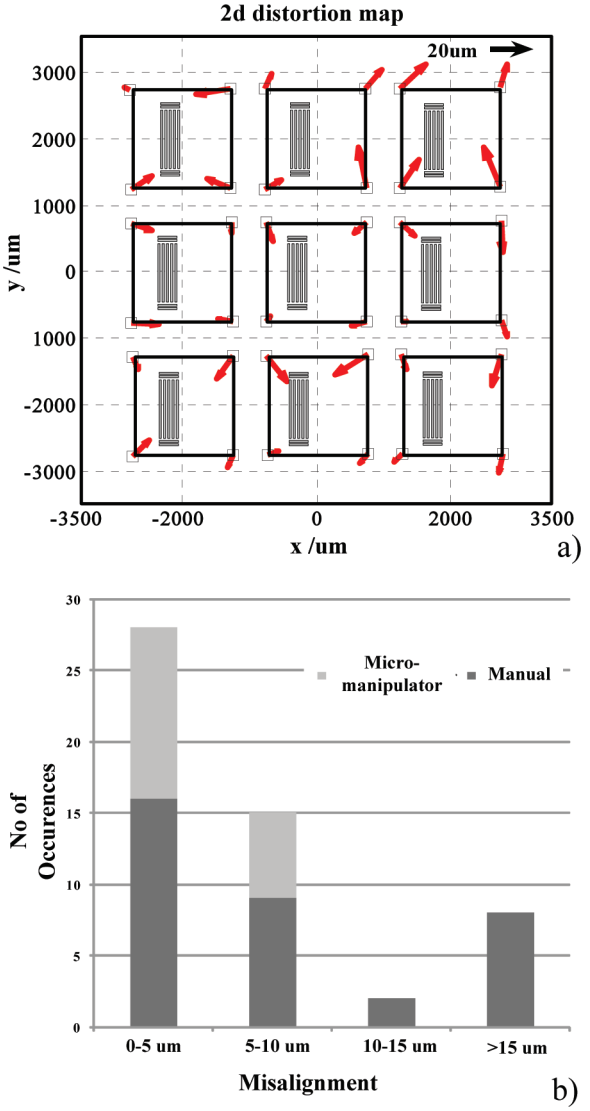

Figure 9. (a) Absolute distortion between the printed images and the silicon master. (b) Distribution of layer-to-layer misalignment.

that is, the difference between the printed image and the silicon master. A six-level print is made as above, and the coordinates of the inner corners of the supporting bars are measured relative to the origin of the 3×3 array. These were used as landmarks because they were easier to measure at that scale. The corresponding measurements were carried out on the original silicon master, and the relative rotation/translation between the two sets of data was corrected. The distortion between the image and the original is presented as a vector map in Figure 9a. The maximum offset noted was 23 μm, and the mean was 11 μm. The offsets appear to be randomly distributed with no clear trend.

Multilevel accuracy was quantified by measuring the center line to center line spacing of the periodic bar images formed from adjacent stamps and subtracting the nominal design value (20 μm). This would give the layer-to-layer misalignment (to ~1 μm accuracy, based on the magnification and the image resolution). The distribution of the misalignment data is presented in Figure 9b and is based on 50 prints in the central cell of the 3 × 3 array. Average misalignments of 9.1 μm (standard deviation of 8.2 μm) are obtained, and the median value is 5.5 μm, suggesting that the misalignments lie mostly in the 0−10 μm range. These values are also consistent with the measured absolute distortion.

For those prints that lie within the 0−5 μm band (Figure 9b), there is hardly any deviation (< 2 μm) in the misalignment within different cells of the array of patterns. For those prints with large misalignment (> 15 μm), the deviation between cells could be as much as 15 μm. Moreover, those stamps that gave inaccuracies of >15 μm tended to do so consistently, and this points toward defects within those stamps due to processing rather than toward the inherent limit of the self-alignment system. In fact, these stamps had curled slightly because of the shearing of the steel backing when they were cut with scissors.

The use of a more controlled actuation is verified by using a linear motion manipulator (PVX 500, Wentworth Laboratories, Ltd., Bedfordshire, England) with the probe tip removed to cause deflection. The average layer-to-layer misalignment then drops to 3.4 μm (with a standard deviation of 3.3 μm), and the median drops to 2.1 μm. The distribution is shown in Figure 9b. These preliminary results indicate that controlled actuation can significantly improve the accuracy.

4.3. Comparison with Previous Work. Despite the large body of work tackling pattern fidelity in μCP, few studies present data regarding multilevel accuracy. Most focus on the difference between the printed image and the original master/stamp, termed absolute distortion. James et al.[23] and Lauer et al.[24] report three-axis stages with alignment optics capable of $\pm$1 μm print-to-print accuracy (for stamp sizes of ~10 × 10 mm). A commercial solution, μCP2.1[25] (Gesim), consists of alignment stages with optics and pneumatic actuation that enables 5 μm positioning accuracy. Others such as Decré et al.[6] and Burgin et al.[5] present high-fidelity contact printers (absolute distortions of 0.69 μm over 100 mm and 1 μm over 75 mm) with alignment optics that presumably allow $\pm$1 μm accuracy from run to run. Rogers et al.[36] present relative alignment data by printing an image on a reference grid, displacing and rotating the stamp, and printing again. After translational and rotational errors are subtracted, the maximum difference between the two prints with respect to the reference grid is reported to be 4 μm over a length of 4.5 mm (0.09%). This reflects the errors that would have occurred even if the prints were perfectly aligned. An approach similar to ours in spirit has been presented by Tien et al.[37] Here, a single stamp with patterns distributed over four levels is designed, and by varying the applied pressure, different areas of the stamp make contact, thereby making complementary, inherently self-aligned patterns. Feature sizes are of the order of 100 μm and no alignment data is presented, but values of tens of micrometers can be inferred from the images. This approach is very simple and easy to implement but requires careful loading, and cross contamination can be an issue as sizes are scaled down.

Our approach, with a layer-to-layer accuracy of 10 μm over a length of 5 mm (0.2%), is relatively inaccurate but still allows multilevel patterning with no overhead such as alignment optics. The complexity of the silicon masters may be of concern, but once these are available, hundreds of stamps can be made by simple replica molding. As for attaching the steel backing to the polymer, we admit that this step is low yield because it requires hand−eye manipulation, and we are currently investigating ways of improving this aspect.

The main drawback in our opinion is that a matching microfabricated substrate is still required. This can be reused by stripping the Au layer and using a fresh coating for new experiments.

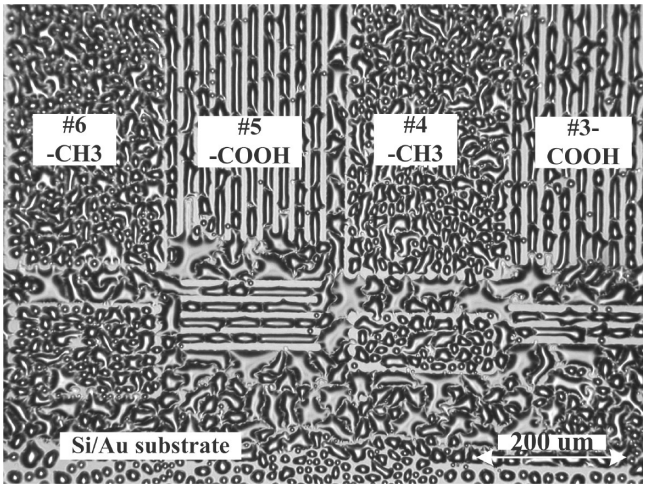

Figure 10. Condensation image revealing the patterns of SAMs with different monolayers. The different droplet distributions on the hydrophilic (−COOH) and hydrophobic (−CH_3) areas provide sufficient contrast for imaging by optical microscopy.

Another avenue to be investigated would be injection/replica molding these substrates and then coating with Au.

4.4. μCP with Different Inks. The patterning of different monolayers is demonstrated using 1-hexadecanethiol ($HS(CH_2)_{15}CH_3$) and 11-mercaptoundecanoic acid ($HS(CH_2)_{10}C0_2H$). Even stamp variants were inked with 0.5 mM hexadecanethiol in ethanol, as before, and odd variants were inked with 1 mM mercaptoundecanoic acid in ethanol.

All six stamps were sequentially aligned and printed onto a single target die as described in section 4.1. For the odd variants carrying the carboxylic acid-terminated thiol, the contact time was increased to ~60 s.

To facilitate imaging, the underivatized Au was etched as in section 4.1 to reveal the SAM-covered regions. Condensation figures were used to differentiate between the hydrophilic and hydrophobic SAMs.[38] The target substrate was cooled after patterning and then exposed to ambient conditions where water vapor would condense. The droplet size distributions differ significantly between regions covered by the two SAMs as shown in Figure 10.

Two different inks were used here as demonstration, but it is clear that up to six different compatible monolayers with different terminations could be patterned by μCP and a seventh monolayer could be deposited from solution onto the empty areas.

5. Conclusions

We have successfully designed, fabricated, and demonstrated a six-level μCP tool with self-alignment features. Multilevel accuracy has been shown to lie within the 5−10 μm range with a manual operating mode and without the need for optical alignment. Areas requiring further investigation are the passive alignment mechanism and its limits and scaling to larger die sizes. The fabrication process also needs to be optimized to enable true wafer-scale processing. In addition, more consistent print actuation mechanisms, such as pneumatic, which would not overly complicate the current setup, warrant further study.

Potential applications lie in the area of biochemistry, where multilevel μCP for sensitizing surfaces (e.g., in a biosensor array or multianalyte biochips) is required. Six-level patterning to impart different biochemical and/or tribological properties to a

(36) Rogers, J. A.; Paul, K. E.; Whitesides, G. M. *J. Vac. Sci. Technol., B* **1998**, *16*, 88–97.
(37) Tien, J.; Nelson, C. M.; Chen, C. S. *Proc. Natl. Acad. Sci. U.S.A.* **2002**, *99*, 1758–1762.
(38) Lopez, G. P.; Biebuyck, H. A.; Frisbie, C. D.; Whitesides, G. M. *Science* **1993**, *260*, 647–649.

substrate has been demonstrated, and more levels could be implemented as required. The polymer molding approach significantly drives down cost and opens new possibilities for patterning in geometrically challenging microstructures such as microchannels.

Most importantly, perhaps, is that reliable aligned multilevel patterning can be carried out without any additional equipment, except for a compatible substrate. A batch fabrication process for structured substrates (e.g., by injection molding and then coating with an appropriate layer) could be envisaged.

Acknowledgment. We thank Dr. M. M. Ahmad and Dr. S. Wright for useful discussions.